Mixture Absorption System of Monoethanolamine–Triethylene Glycol for CO2 Capture

ARTICLE *in* INDUSTRIAL & ENGINEERING CHEMISTRY RESEARCH · FEBRUARY 2011

Impact Factor: 2.59 · DOI: 10.1021/ie101810a

5 AUTHORS, INCLUDING:

Le Du
Beijing University of Chemical Technology
12 PUBLICATIONS **103** CITATIONS

SEE PROFILE

Guangsheng Luo
Tsinghua University
292 PUBLICATIONS **4,236** CITATIONS

SEE PROFILE

I&EC research
Industrial & Engineering Chemistry Research

ARTICLE

pubs.acs.org/IECR

Mixture Absorption System of Monoethanolamine−Triethylene Glycol for CO_2 Capture

Jing Tan, Huawei Shao, Jianhong Xu, Le Du, and Guangsheng Luo*

The State Key Lab of Chemical Engineering, Department of Chemical Engineering, Tsinghua University, Beijing 100084, China

ABSTRACT: In this paper, a mixture system without water but composed of monoethanolamine (MEA) and triethylene glycol (TEG) is designed for CO_2 capture. The solubility of CO_2 in pure TEG and MEA−TEG solutions is determined, respectively, showing that the solubility of CO_2 in TEG is generally consistent with Henry's Law and the value is higher than that in water. The solubility of CO_2 in MEA−TEG solutions significantly increases with the increase of MEA, showing the characteristics of chemical reaction absorption. The absorption mechanism study shows that TEG does not act as a reaction agent. There is only one reaction between CO_2 and MEA. The absence of water in the new system leads to the absence of dissociation of protonated MEA and formation of carbamate ($MEACOO^-$). This is much different from the MEA−water system. A mathematical model is also developed for predicting the solubility of CO_2 in the new system. The results show that the absorption and desorption can be realized at relatively lower temperatures (lower than 353.15 K), which may provide advancement in two aspects: low energy consumption with less solvent evaporation and avoidance of MEA's degradation caused by high-temperature operation.

1. INTRODUCTION

With the global expansion of industrial activities over the past 3 decades, global warming and climate changes are emerging as the important environmental issue of the 21st century.[1] CO_2 is representing about 80% of the greenhouse gases, and fossil-fuel fired power plants are the largest stationary sources of CO_2 emission.[2−4] On the other hand, CO_2 shows an important application value as an industrial raw material, e.g., a refrigerant,[5] and used for CO_2 enhanced oil recovery.[6] As a result, the development of novel technologies for capturing CO_2 from these sources with low energy-consumption and high efficiency is of great importance.

Organic amine (RR′NH) solution is the most widely used absorbent currently for its good performance in the capture of CO_2. When CO_2 comes into contact with an organic amine aqueous solution, the reaction $2RR'NH+CO_2(aq) \rightleftharpoons RR'NH_2^+ + RR'NCOO^-$ takes place, forming a chemical absorption process. Monoethanolamine (MEA) has a high reaction rate with CO_2, and for its low molecular weight it has a much higher absorptive capacity as the same solute weight than other alkaline amines. In the absorption process, the reaction of CO_2 and MEA is shown with the following equation and the heat of absorption is 87.9 kJ/mol of CO_2.[7]

$$2HOC_2H_4NH_2 + CO_2 \rightleftharpoons HOC_2H_4NH_3^+ + HOC_2H_4NHCOO^-$$

However, the application of MEA in aqueous solution as the absorbent for the capture of CO_2 is limited because of the difficulty in the removal of CO_2 from the aqueous MEA solution, which requires high temperature. In an approximate tray-by-tray analysis of an aqueous stripping column for a 17 wt % MEA solution, the assumed conditions for the stripping operation are (1) a pressure of 165.5 kPa (gauge pressure) and a temperature of 388.15 K at the reboiler and (2) a pressure of 137.9 kPa (gauge pressure) and 371.15 K at the top of the column. As shown in Figure 1, there will be 8 theoretical trays and sufficient steam is required to produce 2.1 mol of H_2O per mole of CO_2. It results in a lean solution from the reboiler which contains 0.14 mol of CO_2 per mole of MEA in the leaving stripping section. The heat of vaporization of H_2O is 44 kJ/mol;[8] thus, 92.4 kJ is required to produce 2.1 mol of H_2O steam in order to remove 1 mol of CO_2 from the MEA solution, when the heat of absorption is only 87.9 kJ per mol of CO_2. Therefore, the excessive energy consumption caused by the large amount of water evaporation, the desorption

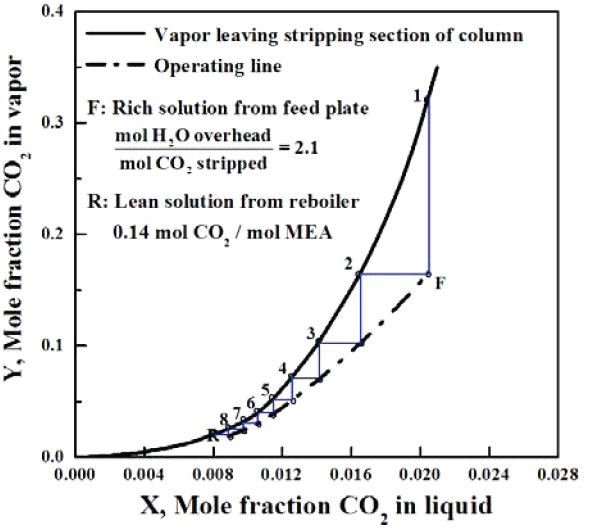

Figure 1. Calculated plate diagram for stripping of CO_2 from aqueous MEA solutions.[9]

Received: August 29, 2010
Accepted: January 18, 2011
Revised: January 7, 2011
Published: March 01, 2011

dx.doi.org/10.1021/ie101810a | *Ind. Eng. Chem. Res.* 2011, 50, 3966–3976

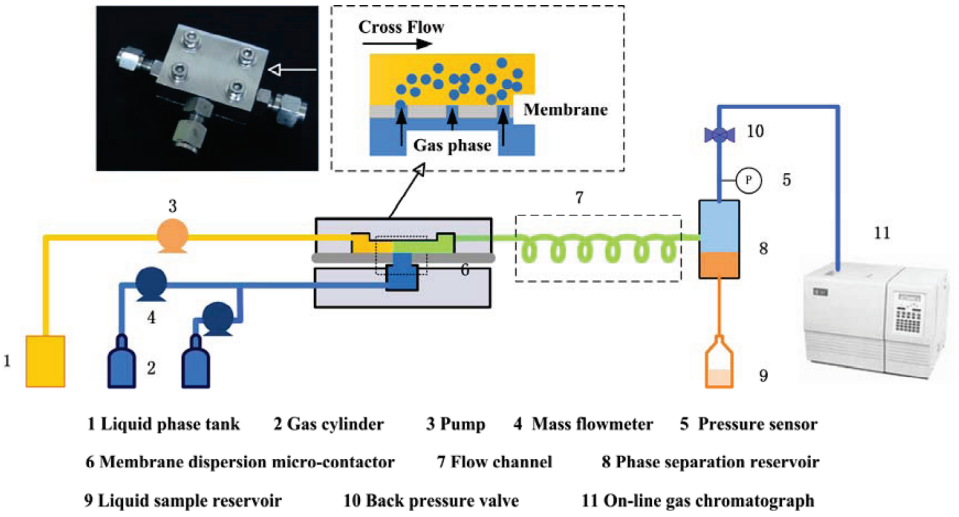

Figure 2. The experimental setup.

of CO_2 is the major factor in constraining the development of using aqueous MEA solutions for CO_2 capture.[9]

Another disadvantage of absorption using aqueous MEA solutions is the loss of MEA during operation. The loss of MEA is mainly caused by thermal degradation[10] and oxidative degradation.[11,12] Studies show that the increase of temperature leads to significant increase of rates of both thermal degradation[10] and oxidative degradation.[13]

As mentioned above, the desorption operation at a higher temperature causes both a large amount of evaporation of water and the degradation of MEA. The dissociation of protonated MEA and the formation of carbamate ($MEACOO^-$) or carbonate in the aqueous environment leads to a more stable combination of CO_2 and solvent and thus a more difficult separation process. They are two main reasons for the high temperature required in the desorption operation. The absence of H_2O may prevent the reaction above and lead to the realization of desorption at lower temperature. Some research[14,15] has been carried out to determine solubility data at 293.15 K of CO_2 in mixtures of organic amines and some organic solvents, such as ethylene glycol (EG), tetrahydrofurfuril alcohol, and *N*-methylpyrrolidone. The results show that compared to the aqueous organic amine solutions, although there is lower CO_2 solubility in liquid, there is a greater difference between CO_2 partial pressure at the equal extent of reaction especially at the small extents, and it may help to complete more regeneration of the absorbent. Some research has also been carried out on the solubility of CO_2 in diethylene glycol (DEG), indicating that the solubility of CO_2 in DEG is significantly higher than in water (the data are shown in Figure 5).[16] The higher solubility of CO_2 as well as the low vapor pressure[17] make glycol, like EG, DEG, and triethylene glycol (TEG), possible to be used as a suitable solvent in CO_2 chemical absorption. Although TEG show higher viscosity than EG and DEG, it may be a suitable solvent for it has a higher degradation temperature than EG and DEG.[18] On the other hand, TEG also shows good stability and miscibility with organic compounds such as aromatics, which makes it used as a general solvent in aromatic extraction processes.

The objective of this work is to develop a mixture system for CO_2 capture with low energy consumption, especially to realize absorbent regeneration at relatively low temperature when monoethanolamine (MEA) is used as the chemical absorbent. As discussed above, TEG is designed as the diluent because of its miscibility with organic amine, low volatility, high boiling point, and high degradation temperature. Thus, a system without water but composed of MEA and TEG is designed as the absorbent to prevent the dissociation of protonated MEA and the formation of carbamate ($MEACOO^-$) or carbonate. The solubility of CO_2 in pure TEG and MEA−TEG solutions is determined, respectively. The modeling and mechanism studies have been carried out. The absorption characteristics with the new system are compared with the traditional MEA−H_2O system.

2. EXPERIMENTAL SECTION

2.1. Materials. Triethylene glycol was analytically pure and purchased from Tianjin Guangfu Fine Chemical Research Institute. Monoethanolamine was analytically pure and purchased from Beijing Chemical Plant. Carbon dioxide (CO_2) and nitrogen (N_2) at 99.995 mol % was purchased from Beijing Huayuan Gas Chemical Industry Co., Ltd.

2.2. Gas−Liquid Equilibrium Measurement. *2.2.1. Measurement Method and Experimental Setup.* In this study, a rapid measurement method is used to determine the CO_2 solubility in pure TEG and solutions of TEG−MEA, using a membrane dispersion microcontactor. The principle and procedures have been described in detail in our previous work.[19]

The experimental setup is shown in Figure 2. The membrane dispersion microcontactor was made with stainless steel. A stainless steel microfiltration membrane with a 5 μm average pore size and 0.3 mm thickness was used as the dispersion medium. The active membrane area was 30 mm^2. The size of the flow channel was 1.5 mm × 2 mm × 3 mm and the size of the gas buffer reservoir was 1.5 mm × 5 mm × 1 mm. In order to maintain the two-phase dispersion and allow for the adjustment of the residence time, a long stainless steel capillary with an inner diameter of 2 mm was connected directly downstream of the microcontactor. Capillary pipes, 40, 90, 190, 290, 390, 490, and 790 cm in length, respectively, were used accordingly to adjust the residence time. A phase separator with an inner diameter of 8 cm and a height of 20 cm was connected with the capillary pipe.

In the measurement, the liquid phase was pumped into the top side of the membrane (the flow channel) while the gas phase was pumped into the gas chamber. The pressure difference caused

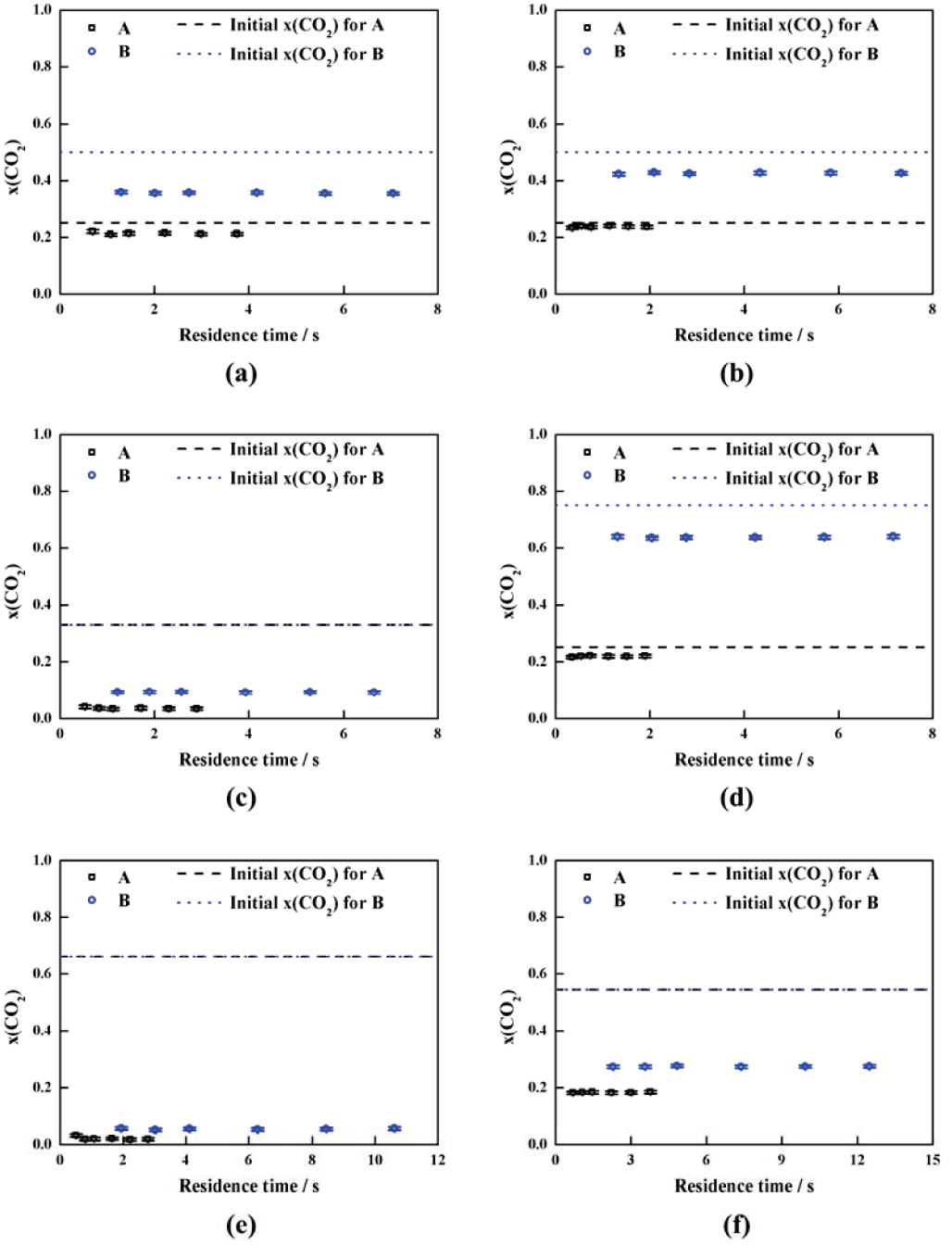

Figure 3. Mole fraction of CO_2, x_{CO_2}, versus residence time. The operating conditions for parts a−f are listed in Table 1.

the gas phase to disperse as microsized bubbles as it passed through the membrane into the liquid phase forming a microdispersion. The microdispersion flowed along the capillary pipe allowing for a sufficient residence time for mass transfer to occur before it flowed into the gas−liquid phase separator. Mass transfer from the gas phase to the liquid phase took place during both the dispersion and flow stage. The gas−liquid microdispersed fluid flowed into the phase separator and immediately separated into the corresponding gas and liquid phases. The separated gas and liquid phases flowed out from the top and bottom portions of the separator, respectively. The gas phase flows from the phase separator immediately into the online gas chromatograph, applying a simple and accurate sampling process.

An advection pump (0−100 mL/min, with a measurement accuracy of ±1%) was used to pump the liquid phase into the microcontactor. Two mass flowmeters (0−500 mL/min of N_2 at 0 °C, 101.325 kPa, with a measurement accuracy of ±1.5%) were used to deliver a gas mixture at stable pressures and flow rates.

A water bath (room temperature to 373.15 °C, with a resolution of ±0.1 K) was used to maintain the temperature of all the feed pipes, the microcontactor, the capillary pipes, and phase separator.

A back pressure valve (0−0.3 MPa range) was used to maintain the outlet pressure of the phase separator at the required pressure. A pressure sensor (0−0.3 MPa, with an accuracy of ±0.5%) was set before the back pressure valve to determine the total pressure of the gas phase.

Table 1. Operation Conditions and Residence Time of Figure 3

	T/K	C_{MEA}/mol/L		Q_{CO_2}/mmol/min	Q_{N_2}/mmol/min	Q_L/mL/min	P/kPa	t_0[b]/s
(a)	303.15	0	A[a]	0.004	0.012	30	85	1.07
			B	0.008	0.008	40	340	1.30
(b)	353.15	0	A[a]	0.004	0.012	30	0	0.36
			B	0.008	0.008	40	360	1.34
(c)	303.15	0.3	A[a]	0.004	0.008	30	0	0.53
			B	0.004	0.008	20	100	1.22
(d)	353.15	0.1	A[a]	0.004	0.012	40	0	0.35
			B	0.012	0.004	40	400	1.32
(e)	303.15	0.5	A[a]	0.008	0.004	40	0	0.80
			B	0.008	0.004	30	400	1.95
(f)	353.15	0.5	A[a]	0.006	0.005	40	150	0.69
			B	0.006	0.005	20	450	2.29

[a] The operating conditions with maximum total flow rate ($Q_{CO_2} + Q_{N_2} + Q_L$) used for each system and accordingly the residence times shown are the shortest times for the same flow channel length. [b] The minimum residence time, t_0, to ensure equilibrium was reached for different operation conditions and working systems.

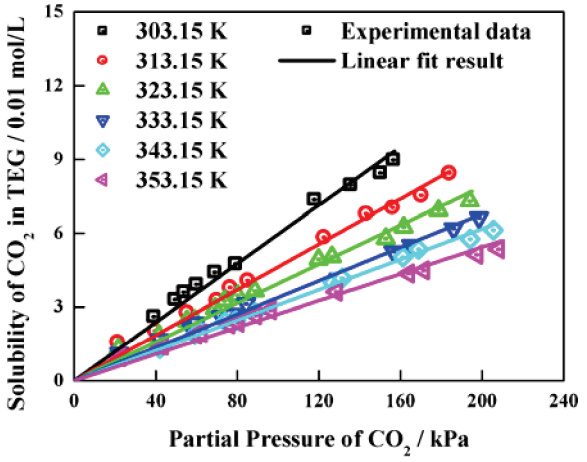

Figure 4. The solubility of CO_2 in pure TEG.

Table 2. Henry Coefficient of CO_2 in TEG at Different Temperature

temperature/K	$H/\times 10^{-6}$ Pa/(mol/L)
303.15	1.68
313.15	2.16
323.15	2.53
333.15	2.95
343.15	3.24
353.15	3.68

After absorption, a gas chromatograph (GC) (Tianmei, 7890 II) using a thermal conductivity detector (TCD) was applied to measure the composition of gas samples online. Gas chromatography measurements were carried out with a carrier gas flow rate of 35 mL/min, a column temperature of 393.15 K, and a detector temperature of 423.15 K. The accuracy of the measurements in the experiments was ±0.5%.

2.2.2. Determination of Solubility Data. Similar to the aqueous systems, N_2 is chosen as an inert gas in this measurement for its much lower solubility than CO_2 in TEG solutions.[20] In this case, once the composition of both gas samples before and after absorption is measured, the amount of gas dissolved in the liquid could be determined by material balance calculations.

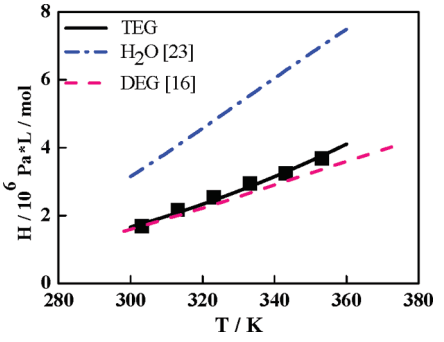

Figure 5. Comparison of the solubility of CO_2 in TEG, DEG, and water.

The small volume of the microcontactor allowed for steady flow to be reached in short time (no more than 2 min). At steady state flow, the amount of CO_2 dissolved in the liquid at certain residence times could be calculated from the analysis of the gas sample using eq 1:

$$\Delta Q_{CO_2} = Q_{CO_2,0} + Q_{N_2} - Q_{N_2}/x_{N_2} \quad (1)$$

where ΔQ_{CO_2} is the amount of CO_2 dissolved in the liquid, moles/minute; $\Delta Q_{CO_2,0}$ is the initial flow rate of CO_2, moles/minute; Q_{N_2} is the flow rate of N_2, moles/minute; x_{N_2} is the mole fraction of N_2 after absorption, moles/moles.

As mentioned in the literature, the boiling point of triethylene glycol is 285 °C at atmospheric pressure,[21] and the vapor pressure of TEG is 2.0048 kPa at 442 K.[22] Thus the evaporation of TEG can be neglected in the measurement. Therefore, the partial pressure of CO_2 after absorption can be calculated as

$$P_{CO_2} = P(1 - x_{N_2}) \quad (2)$$

where P_{CO_2} is the partial pressure of CO_2, kilopascals, and P is the total pressure of gas, measured by the pressure sensor, kilopascals.

2.3. Operation Conditions for Measurement. The gas−liquid microdispersed fluid flows out of the microcontactor and into the subsequent capillary tube. Capillary pipe length was used

dx.doi.org/10.1021/ie101810a |Ind. Eng. Chem. Res. 2011, 50, 3966–3976

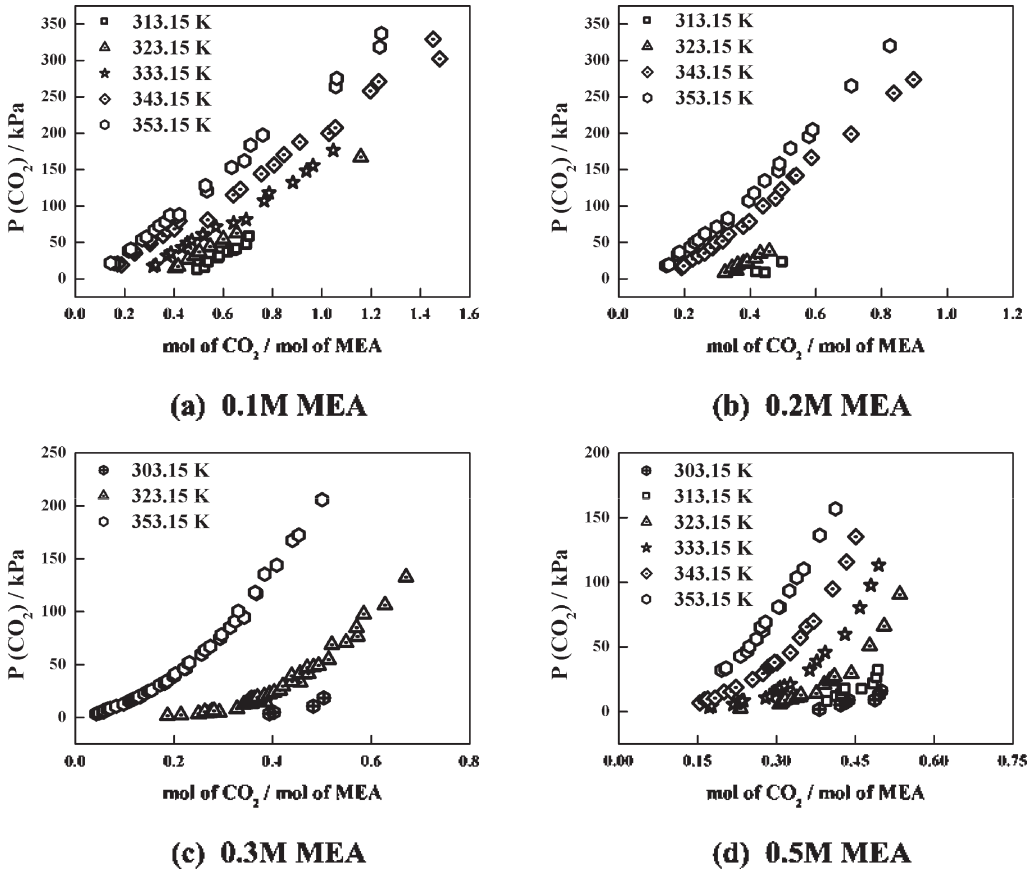

Figure 6. Solubility of CO_2 in MEA−TEG solutions.

to control the residence time, ensuring that the mass transfer time is long enough for equilibrium to be reached. Figure 3 shows plots of the mole fraction of CO_2, x_{CO_2}, versus residence time under different operating conditions. For all six working systems and conditions, x_{CO_2} remained nearly constant at residence times greater than 1.07 s. Here, the values for x_{CO_2} could be considered as the solubility of CO_2 in the solvent.

The operating conditions used and residence times, t_0, to ensure equilibrium was reached are listed in Table 1, showing that t_0 was less than 1.07 s. Thus, within the range of the operation conditions identified here, sufficient mass transfer rate will be provided and vapor−liquid equilibrium will be achieved. The error bars in Figure 3 show the variances of the x_{CO_2} value at different operating times, indicating that the measurement of x_{CO_2} provides good repeatability. In the measurement, the capillary pipe with the length of 490 cm was used, providing sufficient residence time for the gas−liquid system to reach equilibrium.

3. RESULTS AND DISCUSSION

3.1. Solubility of CO_2 in Pure TEG. Figure 4 shows the solubility of CO_2 in pure TEG. It indicates the solubility is proportional to the partial pressure of CO_2 in the vapor phase, generally consistent with Henry's Law:

$$x_B = \frac{p_B}{H_B} \quad (3)$$

where x_B is the solubility of the solute B in the solvent, moles/liter, P_B is the partial pressure in the vapor phase of B, pascals, and H_B is the Henry coefficient, pascal/(moles/liter).

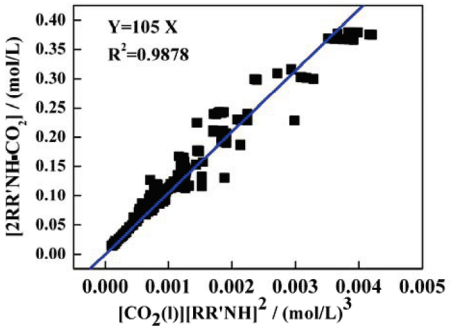

Figure 7. Determination of K_{CO_2} at 353.15 K.

Table 2 shows the Henry coefficient of CO_2 in TEG at different temperatures, proclaiming that H increases with an increase in temperature. The linear fit is carried out by ln H on $1/T$, showing that

$$\ln H = 19.75 - \frac{1628}{T}$$

Figure 5 shows the comparison between the solubility of CO_2 in TEG, DEG, and water, indicating that the solubility of CO_2 in TEG is much higher than in water while similar as in DEG at the same partial pressure of CO_2. The difference is especially greater as the temperature increases.

3.2. Solubility of CO_2 in MEA−TEG Solutions. Figure 6 shows the solubility of CO_2 in MEA−TEG solutions, proclaiming that the CO_2 loading of MEA increases with the vapor pressure of CO_2. At

dx.doi.org/10.1021/ie101810a |Ind. Eng. Chem. Res. 2011, 50, 3966–3976

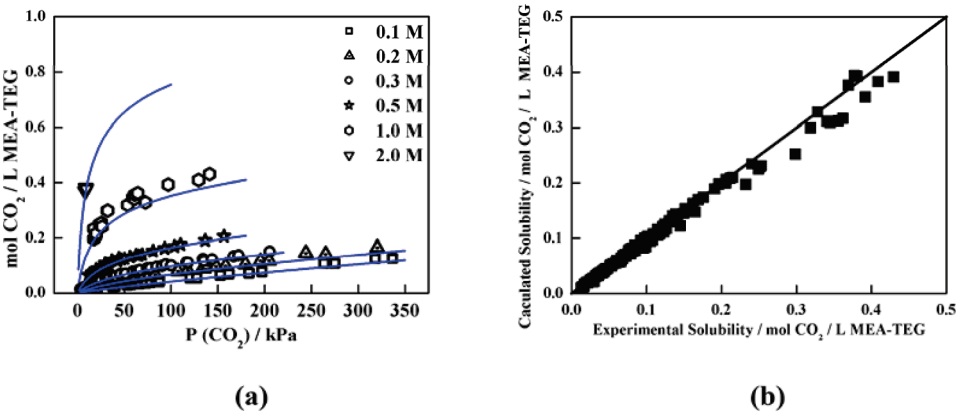

Figure 8. Comparison between model correlation and experimental results at 353.15 K.

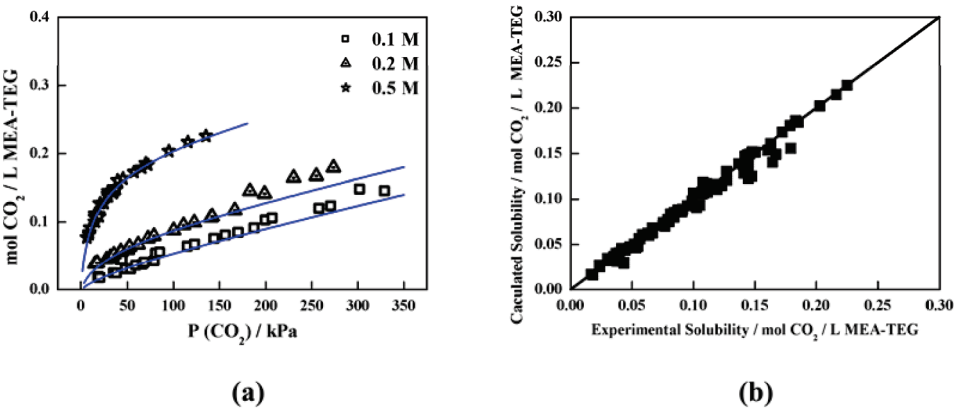

Figure 9. Comparison between the model correlation and experimental results at 343.15 K.

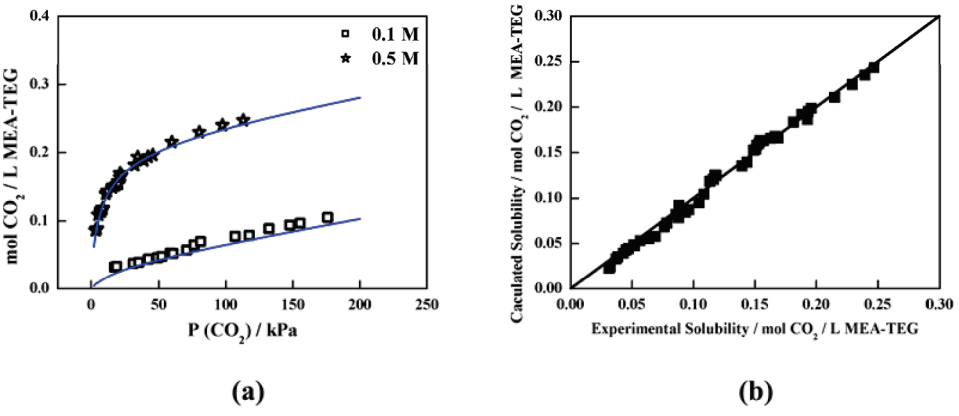

Figure 10. Comparison between the model correlation and experimental results at 333.15 K.

low MEA concentration (lower than 0.2 mol/L) and high temperature (353.15 K), the trend is similar to the physical absorption process, and at high MEA concentration and low temperature, the CO_2 loading curves show a bending trend. These results indicate that at high temperature and low MEA concentration, physical absorption plays a major role in the absorption process, and with a decrease of temperature and increase of the MEA concentration, the chemical reaction shows an obvious effect.

3.3. Absorption Mechanism of the New System. As described in the literature, when CO_2 is absorbed in a MEA aqueous solution, the reaction of CO_2 with MEA can be approximated by a general chemical equilibrium reaction, given that the loading is in the region between 0.02 and 0.48,[24]

$$2RR'NH + CO_2(aq) \overset{K_{CO_2}}{\rightleftharpoons} RR'NH_2^+ + RR'NCOO^- \quad (4)$$

where R is $-C_2H_4OH$ and R′ is $-H$ for MEA.

dx.doi.org/10.1021/ie101810a |*Ind. Eng. Chem. Res.* 2011, 50, 3966–3976

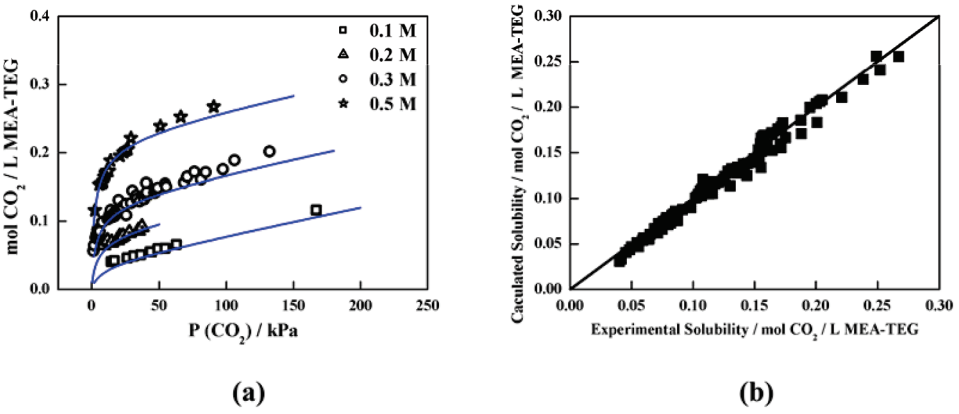

Figure 11. Comparison between the model correlation and experimental results at 323.15 K.

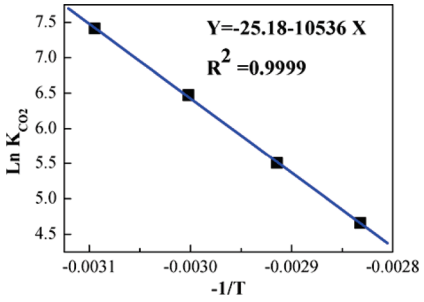

Figure 12. Linear fit of ln K_{co_2} to $-1/T$.

At the same time, the following reactions are taking place in the liquid phase.

$$2H_2O \rightleftharpoons H_3O^+ + OH^- \quad (5)$$

$$CO_2 + 2H_2O \rightleftharpoons H_3O^+ + HCO_3^- \quad (6)$$

$$HCO_3^- + H_2O \rightleftharpoons H_3O^+ + CO_3^{2-} \quad (7)$$

$$RR'NH_2^+ + H_2O \rightleftharpoons H_3O^+ + RR'NH \quad (8)$$

$$RR'NCOO^- + H_2O \rightleftharpoons RR'NH + HCO_3^- \quad (9)$$

When CO_2 is absorbed in a MEA−TEG solution, the reaction written as eqs 5−9 may not occur with the absence of water and dissociation of the alcohol amine salt may also not occur. In other words, only one reaction written as eq 10 occurs in the liquid phase.

$$2RR'NH + CO_2(l) \overset{K_{CO_2}}{\rightleftharpoons} 2RR'NH \cdot CO_2 \quad (10)$$

3.4. Modeling. *3.4.1. Determination of Equilibrium Constant K_{CO_2} at 353.15 K.* With the use of eq 10, an equilibrium constant for the reaction of CO_2 with MEA can be written as

$$K_{CO_2} = \frac{[2RR'NH \cdot CO_2]}{[CO_2(l)][RR'NH]^2} \quad (11)$$

The absorption consists of two parts: physical absorption and chemical absorption. Supposing that (a) chemical absorption does not have an impact on the physical absorption, (b) the physical absorption by MEA can be ignored. Thus physical absorption is proportional to the partial pressure of CO_2 in the gas phase and the volume fraction of TEG in the solutions.

The experimental result shows that no reduction of volume of MEA and TEG after mixing is observed. So the volume fraction of TEG could be calculated as

$$1 - C_{MEA,0}\frac{M_{MEA}}{\rho_{MEA}}$$

where $C_{MEA,0}$ is the concentration of MEA, moles/liter, M_{MEA} is the molecular weight of MEA, 61.08 g/mol, ρ_{MEA} is the density of MEA, which is 1017 g/L at 20 °C.

As a result, the concentration of the species in eq 10 can be calculated as following:

$$[CO_2(l)] = \frac{p_{CO_2}}{H}\left(1 - C_{MEA,0}\frac{M_{MEA}}{\rho_{MEA}}\right) \quad (12)$$

$$[2RR'NH \cdot CO_2] = \Delta C_{CO_2} - [CO_2(l)] \quad (13)$$

$$[RR'NH] = C_{MEA,0} - 2[2RR'NH \cdot CO_2] \quad (14)$$

where ΔC_{CO_2} is the solubility of CO_2 in the MEA−TEG solution, moles/liter.

Inserting the concentrations calculated by eqs 12−14 into eq 11 gives eq 15

$$\Delta C_{CO_2} - \frac{p}{H}\left(1 - C_{MEA,0}\frac{M_{MEA}}{\rho_{MEA}}\right) = K_{CO_2}\frac{P_{CO_2}}{H}\left(1 - C_{MEA,0}\frac{M_{MEA}}{\rho_{MEA}}\right)\left\{C_{MEA,0} - 2\left[\Delta C_{MEA} - \frac{p_{CO_2}}{H}\left(1 - C_{MEA,0}\frac{M_{MEA}}{\rho_{MEA}}\right)\right]\right\}^2 \quad (15)$$

Equation 15 shows that the chemical equilibrium constant K_{CO_2} can be determined by linear fitting as P_{CO_2} and ΔC_{CO_2} are determined in the experiments.

As shown in Figure 7, K_{CO_2} at 353.15 K can be determined to be 105, by $[2RR'NH \cdot CO_2]$ on $[CO_2(l)][RR'NH]^2$ for the linear fit.

Then, an explicit equation is solved for the solubility of CO_2 in the MEA−TEG solution at 353.15 K to verify the accuracy of K_{CO_2}.

Figure 8 shows a comparison between the model correlation and the experimental results for the solubility of CO_2 in the

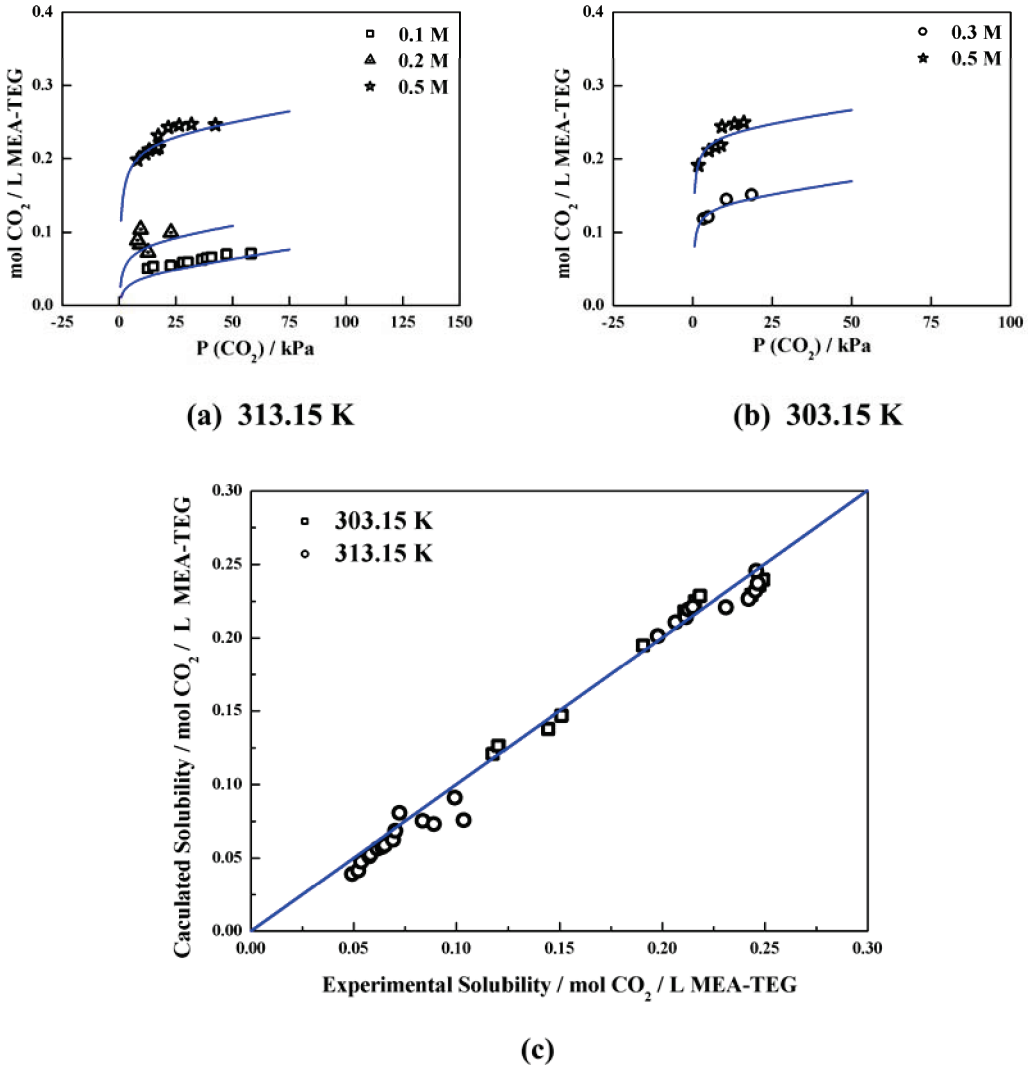

Figure 13. Comparison between the model correlation and experimental results at 313.15 K and 303.15 K.

MEA−TEG solution. It can be seen that the correlation gives satisfactory results over the partial pressure of CO_2 in our experiments.

3.4.2. Determination of K_{CO_2} at 343.15 K, 333.15 K, and 323.15 K. In accordance with the method as mentioned in section 3.4.1, the chemical equilibrium constants at 343.15 K, 333.15 K, and 323.15 K are determined to be 245, 655, and 1650, respectively. Figures 9−11 show the good agreement between the model correlation and the experimental results for the solubility of CO_2 in the MEA−TEG solution.

3.4.3. Heat of Absorption of CO_2. Stating from the Gibbs−Helmholtz equation:

$$\left[\frac{\partial}{\partial T}\left(\frac{\Delta G}{T}\right)\right]_P = -\frac{\Delta H}{T^2} \tag{16}$$

Assuming that K_{CO_2} is affected little by pressure, eq 16 can be derived for the temperature dependence of K_{CO_2}:

$$\frac{\mathrm{d}(\ln K_{CO_2})}{\mathrm{d}\left(-\frac{1}{T}\right)} = \frac{\Delta H}{R} \tag{17}$$

As shown in Figure 12, the linear fit has been carried out by ln K_{CO_2} on $-1/T$, and K_{CO_2} can be predicted by the following equation:

$$K_{CO_2} = \exp\left(-25.18 + \frac{10\,536}{T}\right) \tag{18}$$

With the derivative of eq 18, the heat of absorption is calculated as

$$\Delta H = R\frac{\mathrm{d}(\ln K_{CO_2})}{\mathrm{d}\left(-\frac{1}{T}\right)}$$

As calculated in Figure 12,

$$\frac{\mathrm{d}(\ln K_{CO_2})}{\mathrm{d}\left(-\frac{1}{T}\right)} = -10\,536$$

dx.doi.org/10.1021/ie101810a |*Ind. Eng. Chem. Res.* 2011, 50, 3966–3976

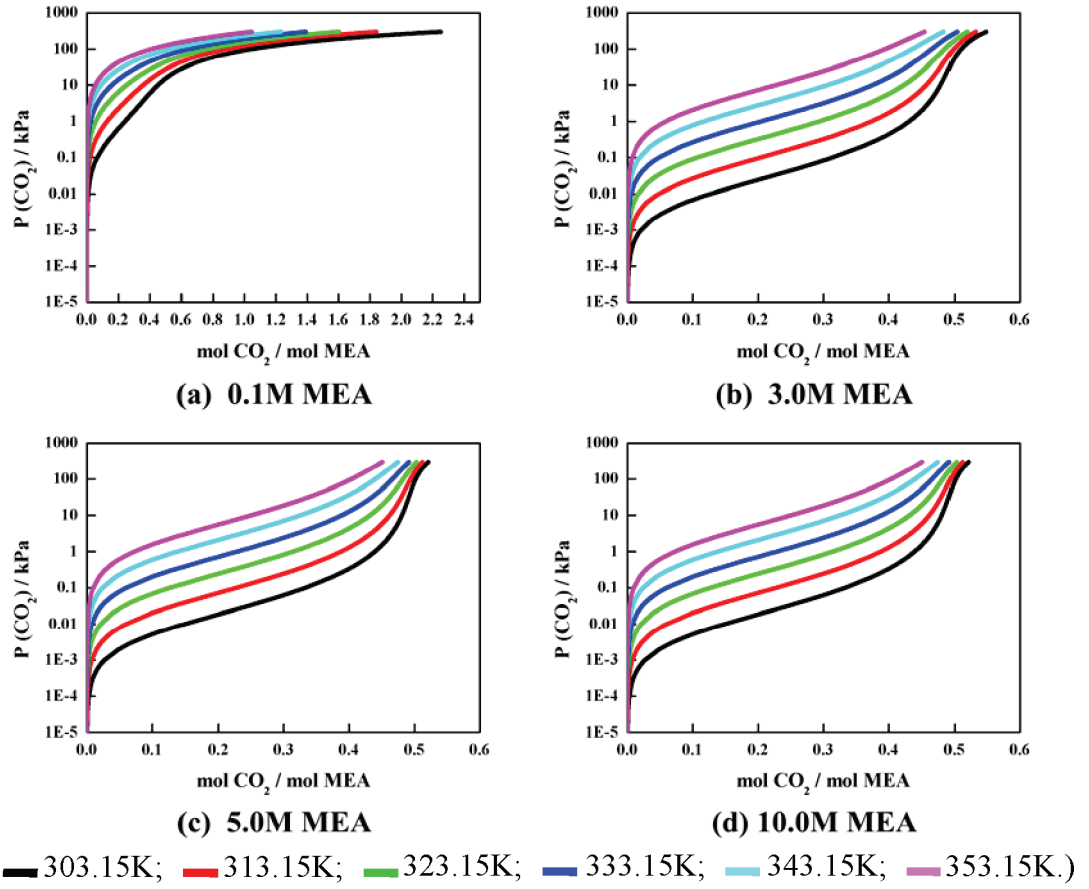

Figure 14. Calculated CO_2 loading of MEA at different concentrations.

Table 3. Reasonable Operation Range Analysis for MEA−TEG System

C (MEA)/ mol/L	temperature/ K	P (CO_2)/ kPa	α mol of CO_2/ mol of MEA	mmol of CO_2/ g of absorbent
3.0	303.15	100	0.510	0.31
	353.15	100	0.395	
	353.15	200	0.433	0.56
	353.15	10	0.227	
5.0	303.15	100	0.502	0.45
	353.15	100	0.404	
	353.15	200	0.435	0.85
	353.15	10	0.250	
10.0	303.15	100	0.496	0.84
	353.15	100	0.407	
	353.15	200	0.434	1.63
	353.15	10	0.261	

Therefore, the heat of absorption is

$$\Delta H = 87.60\ \text{kJ/mol of } CO_2$$

3.4.4. Prediction with the Model. As derived in sections 3.4.2 and 3.4.3, the solubility of CO_2 in the MEA−TEG solution can be predicted at a particular P_{co_2} and temperature T. According to eq 18, the chemical equilibrium constant K_{co_2} is determined to be 4730 at 313.15 K and 14 350 at 303.15 K. Figure 13 shows a good agreement between the model correlation and the experimental results for the solubility of CO_2 in the MEA−TEG solution at 313.15 K and 303.15 K.

3.5. Prediction of Reasonable Operation Range. In section 3.3, the reaction mechanism of CO_2 absorption in the MEA−TEG solution is analyzed, and this mechanism is verified in section 3.4 by calculating the chemical equilibrium constant K_{co_2} and the heat of absorption. Therefore, the CO_2 loading of MEA can be expressed as a function of the CO_2 partial pressure and the initial concentration of MEA at a specific temperature.

Figure 14 shows the CO_2 loading of MEA at different MEA concentrations, pointing out that the loading is sensitive to the changes of vapor pressure of CO_2 and temperature. These two factors affect the chemical reaction equilibrium through the change in the physical absorption of CO_2. The decrease of temperature and increase of partial pressure of CO_2 lead to higher physical absorption and thus promote the chemical reaction equilibrium moving to carbon dioxide absorption; the increase of temperature and decrease of partial pressure of CO_2 lead to lower physical absorption and thus promotes the chemical reaction equilibrium moving to CO_2 desorption.

Figure 14 also shows the reasonable operation range of this system, taking 5.0 M MEA−TEG (the mass fraction of MEA is 28%) as an example; two operation modes will provide a high loading difference: keeping a certain temperature, realizing absorption at a high vapor pressure, and desorption at a low vapor pressure or keeping a certain vapor pressure, realizing absorption at low temperature, and desorption at high temperature. The CO_2 loading of MEA at different MEA concentrations is listed in Table 3, indicating that the former operation mode

dx.doi.org/10.1021/ie101810a |*Ind. Eng. Chem. Res.* 2011, 50, 3966–3976

may provide a higher CO_2 capture amount within each operation round. As mentioned above, only one chemical reaction takes place in the operation process because of the absence of water; thus, once the operation mode of keeping a certain temperature and changing the vapor pressure is chosen, the energy consumption can be approximately considered as consumption of reaction heat. Assuming the operation condition is the concentration of MEA in TEG is 5.0 mol/L, the temperature is kept at 353.15 K, and the vapor pressure for absorption and desorption are 200 and 10 kPa, respectively, the energy consumption will be around 1990 kJ/kg of CO_2 because the evaporation of TEG and MEA can nearly be neglected.

The realization of absorption and desorption at low temperature and the absence of water may provide advancement in two aspects: low energy consumption with less solvent evaporation and avoidance of MEA's degradation caused by high-temperature operation, showing high potential in the development in CO_2 capture. Of course for its industrial application, further study is required, such as selectivity, special equipment for this system, as well as the influence of water content in the flue gas.

4. CONCLUSIONS

In this paper, a mixture system without water but composed of MEA and TEG is designed as an absorbent of CO_2 with low energy consumption. The solubility of CO_2 in TEG and MEA−TEG solutions is determined, respectively. The solubility of CO_2 in TEG shows characteristics of physical absorption, which is generally consistent with Henry's Law and is smaller than it is in water at the same vapor pressure of CO_2. The solubility of CO_2 in MEA−TEG solutions significantly increases with the increase in MEA concentration, showing the characteristics of the chemical reaction.

The absorption mechanism study was carried out, showing that TEG does not act as a reaction agent and there is only one reaction between CO_2 and MEA. The absence of water leads to the absence of dissociation of protonated MEA and formation of carbamate ($MEACOO^-$). A mathematical model is also developed for predicting the solubility of CO_2 in the new system.

According to the mathematical model, analysis for the reasonable operation method for the MEA−TEG system was carried out. Keeping a certain temperature while changing the partial pressure and keeping a certain partial pressure while changing the temperature will both realize CO_2 capture. The former operation mode may have better performance. The capture amount will reach 1.63 mmol of CO_2/g of absorbent at the temperature of 353.15 K.

The realization of absorption and desorption at low temperature and the absence of water may provide advancement in two aspects: low energy consumption with less solvent evaporation and avoidance of MEA's degradation caused by high-temperature operation, showing the high potential in the development in CO_2 capture.

AUTHOR INFORMATION

Corresponding Author

*E-mail: gsluo@tsinghua.edu.cn. Tel.: +86-10-62783870. Fax: +86-10-62783870.

ACKNOWLEDGMENT

We would like to acknowledge the support of the National Natural Science Foundation of China (Grants 20876084 and 21036002) and the Chinese National Programs for High Technology Research and Development (Grant 2008AA062301) for this work.

REFERENCES

(1) Herzog, H.; Eliasson, B.; Kaarstad, O. Capturing greenhouse gases. *Sci. Am.* **2000**, *282*, 72.

(2) Faiz, R.; Al-Marzouqi, M. Mathematical modeling for the simultaneous absorption of CO_2 and H_2S using MEA in hollow fiber membrane contactors. *J. Membr. Sci.* **2009**, *342*, 269.

(3) Desideri, U.; Paolucci, A. Performance modelling of a carbon dioxide removal system for power plants. *Energy Convers. Manage.* **1999**, *40*, 1899.

(4) Berger, A. Global warming 2001. *J. Phys. IV* **2002**, *12*, 19.

(5) Crabb, C. Versatile CO_2 continues to expand into new geographic markets and industrial applications. *Chem. Eng. (N.Y., NY, U.S.)* **2000**, *107*, 49.

(6) Steeneveldt, R.; Berger, B.; Torp, T. A. CO_2 capture and storage - Closing the knowing-doing gap. *Chem. Eng. Res. Des.* **2006**, *84*, 739.

(7) Gabrielsen, J.; Michelsen, M. L.; Stenby, E. H.; Kontogeorgis, G. M. A model for estimating CO_2 solubility in aqueous alkanolamines. *Ind. Eng. Chem. Res.* **2005**, *44*, 3348.

(8) Song, C. H. Overview of hydrogen production options for hydrogen energy development, fuel-cell fuel processing and mitigation of CO_2 emissions. *Proceedings of 20th International Pittsburgh Coal Conference*, Pittsburgh, PA, USA, Sept. 15−19, 2003; pp 40−43.

(9) Kohl, A. L.; Riesenfeid, F. C. *Gas Purification*; Gulf Publishing Company: Houston, TX, 1985.

(10) Bello, A.; Idem, R. O. Comprehensive study of the kinetics of the oxidative degradation of CO_2 loaded and concentrated aqueous monoethanolamine (MEA) with and without sodium metavanadate during CO_2 absorption from flue gases. *Ind. Eng. Chem. Res.* **2006**, *45*, 2569.

(11) Chi, S.; Rochelle, G. T. Oxidative degradation of monoethanolamine. *Ind. Eng. Chem. Res.* **2002**, *41*, 4178.

(12) Sexton, A. J.; Rochelle, G. T. Catalysts and inhibitors for oxidative degradation of monoethanolamine. *Int. J. Greenhouse Gas Control* **2009**, *3*, 704.

(13) Bello, A.; Idem, R. O. Pathways for the formation of products of the oxidative degradation of CO_2-loaded concentrated aqueous monoethanolamine solutions during CO_2 absorption from flue gases. *Ind. Eng. Chem. Res.* **2005**, *44*, 945.

(14) Semenova, T. A., Leites, I. L., Eds. *Purification of Technological Gases*; Chimia: Moscow, 1977.

(15) Leites, I. L. Thermodynamics of CO_2 solubility in mixtures monoethanolamine with organic solvents and water and commercial experience of energy saving gas purification technology. *Energy Convers. Manage.* **1998**, *39*, 1665.

(16) Jou, F. Y.; Otto, F. D.; Mather, A. E. Solubility of H_2S and CO_2 in diethylene glycol at elevated pressures. *Fluid Phase Equilib.* **2000**, *175*, 53.

(17) Wu, H.; Chung, T. W. Influences for the addition of ethanol to the absorption system on the interfacial disturbances and mass transfer performance. *Ind. Eng. Chem. Res.* **2008**, *47*, 7397.

(18) Bahadori, A.; Vuthaluru, H. B.; Mokhatab, S. Analyzing solubility of acid gas and light alkanes in triethylene glycol. *J. Nat. Gas Chem.* **2008**, *17*, 51.

(19) Tan, J.; Xu, J. H.; Wang, K.; Luo, G. S. Rapid measurement of gas solubility in liquids using a membrane dispersion micro-contactor. *Ind. Eng. Chem. Res.* **2010**, *49*, 10040.

(20) Gainar, I.; Anitescu, G. The solubility of CO_2, N_2 and H_2 in a mixture of dimethylether polyethylene glycols at high-pressures. *Fluid Phase Equilib.* **1995**, *109*, 281.

(21) Steele, W. V.; Chirico, R. D.; Knipmeyer, S. E.; Nguyen, A. Measurements of vapor pressure, heat capacity, and density along the saturation line for epsilon-caprolactam, pyrazine, 1,2-propanediol, triethylene glycol, phenyl acetylene, and diphenyl acetylene. *J. Chem. Eng. Data* **2002**, *47*, 689.

(22) Orliac, O.; Rouilly, A.; Silvestre, F.; Rigal, L. Effects of various plasticizers on the mechanical properties, water resistance and aging of thermo-moulded films made from sunflower proteins. *Ind. Crops Prod.* **2003**, *18*, 91.

(23) Li, M. H.; Chang, B. C. Solubilities of carbon dioxide in water + monoethanolamine + 2-Amino-2-methyl-1-propanol. *J. Chem. Eng. Data* **1994**, *39*, 448.

(24) Astarita, G. *Mass Transfer with Chemical Reactions*; Elsevier Publishing Company: Amsterdam, The Netherlands, 1967.